Disruption of HDAC/CoREST/REST repressor by dnREST reduces genome silencing and increases virulence of herpes simplex virus

Te Du[1], Guoying Zhou[1], Shaniya Khan, Haidong Gu, and Bernard Roizman[2]

Marjorie B. Kovler Viral Oncology Laboratories, The University of Chicago, Chicago, IL 60637

Contributed by Bernard Roizman, July 28, 2010 (sent for review July 1, 2010)

In nonneuronal cells, herpes simplex virus 1 overcomes host defenses, replicates, and ultimately kills the infected cell. Among the host defenses suppressed by the virus is a repressor complex whose key components are histone deacetylase (HDAC) 1 or 2, RE-1 silencing transcription factor (REST), corepressor of REST (CoREST), and lysine-specific demethylase (LSD) 1. In neurons innervating cells at the portal of entry into the body, the virus establishes a "latent" infection in which viral DNA is silenced with the exception of a family of genes. The question posed here is whether the virus hijacks this repressor complex to silence itself in neurons during the latent state. To test this hypothesis, we inserted into the wild-type virus genome a wild-type REST [recombinant (R) 111], a dominant-negative REST (dnREST) lacking the N- and C-terminal repressor domains (R112), or an insertion control consisting of tandem repeats of stop codons (R113). The recombinant virus R112 carrying the dnREST replicated better and was more virulent than the wild-type parent or the other recombinant viruses when administered by the corneal or i.p. routes. Moreover, in contrast to other recombinants, corneal route inoculation by R112 recombinant virus resulted in higher DNA copy numbers, higher levels of infectious virus in eye, trigeminal ganglion, or brain, and virtually complete destruction of trigeminal ganglia in mice that may ultimately succumb to infection. These results support an earlier conclusion that the HDAC/CoREST/REST/LSD1 repressor complex is a significant component of the host innate immunity and are consistent with the hypothesis that HSV-1 hijacks the repressor to silence itself during latent infection.

chromatin remodeling | herpesviruses | latency

Herpes simplex virus 1 (HSV-1) replicates at the portal of entry into the body, infects sensory nerve endings, and is transported retrograde to the neuronal nucleus (reviewed in ref. 1). In mice, a common animal model system, the virus replicates in some neurons but is silenced and establishes a latent infection in other neurons. Thus, infectious virus is readily detected during the first 10–15 d after infection at a peripheral site. It then disappears, and by day 28 only latent virus is present in the ganglia. One explanation for the two different outcomes of infection is that on release of the viral DNA into the nucleus, the cell attempts to silence the DNA. This attempt leads to a silent, latent infection in neurons but not in cells at the portal of entry into the body or in cell cultures in which the virus replicates. The fundamental question posed in the studies reported here is whether the silencing system suppressed by the virus in productively infected cells is enabled to establish a silent, "latent" infection in neurons.

Specifically, several lines of evidence indicate that in infected cells, ICP0, an α (immediate-early) protein, plays a crucial role in enabling viral replication at low multiplicities of infection. At the portal of entry, the genes encoding α proteins are activated by a viral protein (α-TIF or VP16) brought into the cell during infection in conjunction with cellular proteins Oct1, HCF1, and a complex of proteins containing lysine-specific demethylase (LSD) 1 (1, 2). This enables the expression of α (immediate-early) genes but, at low multiplicities of infection in the absence of ICP0, viral replication is arrested and the DNA is silenced (3, 4). The cellular silencing factor identified to date is a repressor complex whose major components are histone deacetylase (HDAC) 1 or 2, RE-1 silencing transcription factor (REST), corepressor of REST (CoREST), and LSD1 (5, 6). ICP0 interacts with CoREST (7). In infected cells in the presence of ICP0, HDAC1 is displaced from the CoREST/REST/LSD1 complex (7, 8). Subsequently, HDAC1, CoREST/REST, and LSD1 are at least in part translocated from the nucleus to the cytoplasm (7). The two lines of evidence that support the role of the suppressor complex in arresting viral infection in cells infected with ΔICP0 mutant virus are that (*i*) HDAC inhibitors partially overcome the arrest (9) and (*ii*) replacement of ICP0 with a dominant-negative CoREST that does not bind HDAC1 compensates in a cell-type-dependent manner for the absence of ICP0 (8).

To test the hypothesis that HSV hijacked the same or a related suppressor complex to silence itself, we inserted into the DNA of the wild-type virus a gene encoding a mutated REST flanked by an SV40 promoter and poly(A) signal. The mutated REST lacks the repressor domains located at the N and C termini of the protein (10). The expectation was that the mutated REST would act as a dominant-negative factor and displace wild-type REST but fail to engage HDACs, CoREST, LSD1, and other proteins essential for silencing viral DNA. As a consequence, the virus would multiply in many more neurons and therefore there would be fewer neurons harboring latent virus. We did observe a higher level of replication in the mouse trigeminal ganglia (TG) following corneal inoculation. To our surprise, but not inconsistent with our hypothesis, the recombinant virus turned out to be more virulent than the parent virus from which it was derived.

Results

Construction of Recombinant Viruses. A schematic representation of the functional domains of the REST protein is shown in line 1 of Fig. 1. To construct dominant-negative REST (dnREST), we deleted the codons encoding residues 1–83 and 1008–1097. The dnREST and wild-type (W-T) REST were flanked by the SV40 promoter and poly(A) sequence, respectively. These constructs and the insert control consisting of four stop codons flanked by the SV40 promoter and poly(A) sequence were inserted between U_L3 and U_L4 genes. The resulting viruses were designated R111 (W-T REST), R112 (dnREST), and R113 (insert control). The construction and verification of the inserted DNA sequences were done as described in *Materials and Methods*.

Virus Encoding dnREST Replicates to Higher Titers in Mice and Is More Virulent than the Wild-Type Virus. We report three series of experiments. In the first series of experiments, mice in groups of

Author contributions: B.R., G.Z. and H.G. designed research; T.D., G.Z., S.K., and H.G. performed research; B.R. analyzed data; and B.R. wrote the paper.

The authors declare no conflict of interest.

[1]T.D. and G.Z. contributed equally to this work.

[2]To whom correspondence should be addressed. E-mail: bernard.roizman@bsd.uchicago.edu.

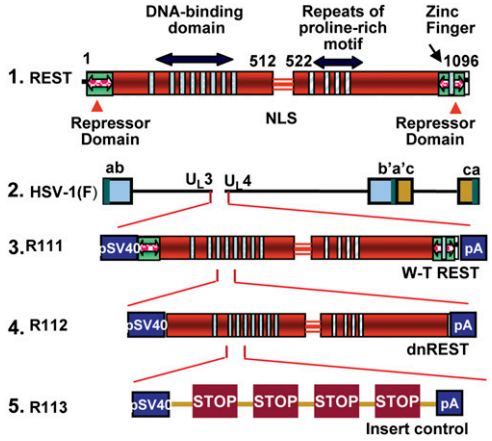

Fig. 1. Schematic representation of the functional domains of wild-type and dominant-negative REST and of the insertion control sequences inserted into the wild-type viral genome. Line 1: arrangement of REST drawn according to ref. 10. Line 2: DNA sequence arrangement of HSV-1 DNA. Line 3: schematic representation of wild-type REST flanked by the SV40 promoter and poly(A) sequence. Line 4: schematic representation of the dominant-negative REST shown lacking the repressor domains and N and C termini. Line 5: sequence arrangement of the insertion control sequence consisting of four stop codons, flanked by the SV40 promoter and poly(A) sequence. All constructs were inserted between U_L3 and U_L4 genes. NLS, nuclear localization signal.

six were inoculated with 10^5 pfu of R111, R112, or R113 mutant viruses by the corneal route. The mice were killed on days 1, 7, 14, or 30. The eyes and TG harvested on days 1, 7, and 14 were assayed for infectious virus. The results (log mean titers) are shown in Fig. 2 *A* and *B*. Viral DNA copy numbers per 50 ng of total DNA isolated from TG harvested on days 1, 7, 14, and 30 after virus inoculation are shown in Fig. 2*C*. The results of these experiments were as follows.

(*i*) In the eye, all three viruses declined to undetectable levels by day 14. The key difference was that on day 7 after inoculation, the titer of R112 was at least 1,000-fold higher than those of R111 or R113 recombinant virus.

(*ii*) The highest yields of infectious virus in TG were detected on day 7. R111 and R113 recombinant virus titers declined to barely detectable levels by day 14. The titers of R112 were higher than those of R111 or R113 recombinant viruses in TG harvested on days 7 and 14.

(*iii*) The viral DNA copy number reflects more accurately the sum total of virus activity in TG. The results (Fig. 2*C*) show that the highest viral DNA copy numbers were obtained on day 7 and declined thereafter. On day 7, the yields of R112 mutant virus DNA were >10-fold higher than those of R111 or R113 mutant virus. All remaining mice infected with R112 succumbed to infection between days 12 and 14. In mice infected with the R111 or R113 mutant virus, the viral DNA copy number decreased slightly between days 14 and 30.

In the second series of experiments, mice were inoculated by the corneal route with 3×10^3 pfu of either R112 or R113. Even at the reduced dose, three of the mice inoculated with R112 succumbed to infection between 9 and 14 d after inoculation. The mice infected with R113 and the surviving mice inoculated with R112 recombinant virus were killed on days 1, 7, 14, 30, or 60 and viral DNA copy number was determined. The DNA copy number per 50 ng of total DNA is shown in Table 1. To compare the results of the experiment, the DNA copy numbers were normalized with respect to the amounts detected in TG on day 1 after inoculation (Fig. 3). The salient features of the results are twofold. In this

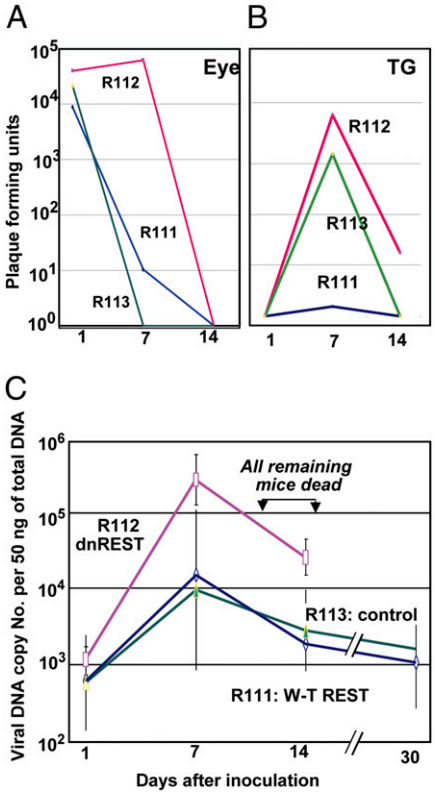

Fig. 2. Quantification of infectious virus and viral DNA copies in the eye and trigeminal ganglia of mice inoculated with 10^5 pfu of virus per eye by the corneal route. (*A* and *B*) Eyes and TG were removed from euthanized mice, homogenized, and plated on Vero cell monolayers. The results shown are geometric mean titers. (*C*) The number of viral DNA copies per 50 ng of DNA was determined by quantitative PCR as described in *Materials and Methods*. The numbers shown are geometric mean titers based on assays of individual ganglia. Note that six mice inoculated with R112 recombinant virus succumbed to infection between days 12 and 14 after infection.

experiment, R112 recombinant virus DNA increased on day 7 and remained relatively unchanged through day 30 and then precipitated to near undetectable levels by day 60. By contrast, the levels of R113 DNA steadily decreased to day 30 and remained relatively stable thereafter.

In the third series of experiments, we examined in greater detail the replication of R112 mutant virus in the eye and brain as compared with that of the wild-type parent virus HSV-1(F). Mice in groups of three were inoculated with 10^5 pfu of either HSV-1(F), R111, or R112 per eye by the corneal route. The eyes and brains were harvested on days 1, 3, 5, 7, 9, 11, and 14 after infection. The results may be summarized as follows.

As shown in Fig. 4*A*, the highest yields of all three viruses were recovered from the eye 1 d after inoculation (Fig. 4*A*). The amounts of R111 mutant virus and those of HSV-1(F) declined and were no longer detectable by day 9. As in the experiment

Table 1. Viral DNA copy number per 50 ng of total DNA

Day	R112	R113
1	$10^{2.9 \pm 0.3}$	$10^{4.0 \pm 0.3}$
7	$10^{3.5 \pm 1.2}$	$10^{3.7 \pm 0.8}$
14	$10^{3.4 \pm 0.9}$	$10^{3.3 \pm 0.7}$
30	$10^{3.5 \pm 1.0}$	$10^{2.3 \pm 0.7}$
60	$10^{<1.5}$	$10^{2.0}$

The mice were inoculated with 3×10^3 pfu by corneal route.

MICROBIOLOGY

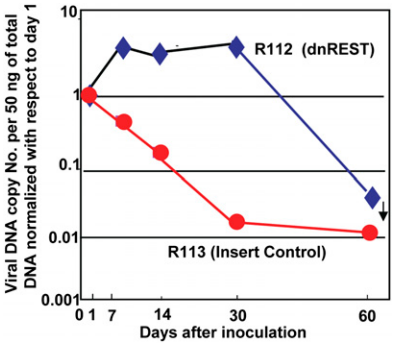

Fig. 3. Quantification of viral DNA copies per 50 ng in TG of mice inoculated by the corneal route with 3×10^3 pfu of R112 or R113 recombinant virus. The assays were done on right ganglia harvested from six mice at each time point. For comparison, in this figure, the DNA copy numbers were normalized with respect to amounts detected on day 1 after virus inoculation on the cornea. The actual geometric mean averages of DNA copy number per 50 ng of DNA are shown in Table 1. Note that in this experiment, three of the mice inoculated with R112 succumbed to infection between days 9 and 14.

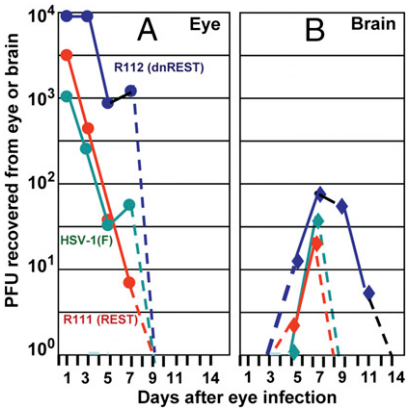

Fig. 4. Quantification of infectious HSV-1 recovered from eyes and brains following inoculation by the corneal route of 10^5 pfu of wild-type parent virus [HSV-1(F)] or R111 or R112 recombinant viruses. The left eyes and brains were removed from euthanized mice, homogenized, and assayed on Vero cell monolayers. The results shown are geometric mean averages of virus recovered from six mice at each time point.

illustrated above, R112 mutant viruses yielded higher amount of infectious virus through day 7 and also declined to undetectable levels by day 9 (Fig. 4*A*).

The amounts of virus recovered from brains of inoculated animals are shown in Fig. 4*B*. The key findings are that both R111 and the wild-type virus were detected in very small amounts only on days 5 and 7. In contrast, the R112 mutant virus was detected in higher amounts on both days 5 and 7 but also on days 9 and 11. No infectious virus was detected on day 14 after inoculations.

REST Was Detected in Murine Trigeminal Neurons. We report three series of experiments. In the first, we examined sections of TG harvested from uninfected mice or mice inoculated with R112 mutant 7 d earlier. The TG were fixed and stained with antibody against REST kindly provided by G. Mandel (Oregon Health & Science University, Portland, OR) or purchased from Novus Biologicals. Examination of the sections (Fig. 5*A*) revealed the presence of REST and changes in the shape of virtually all neurons of TG harvested from mice inoculated with the R112 mutant virus expressing dnREST. REST antigen was detected in both nuclei and cytoplasm (Fig. 5 *A*3 and *A*4). The results demonstrable with both antibodies suggest that by day 7, virtually the entire trigeminal ganglion was infected and in various stages of degeneration.

TG of mock-infected mice showed the presence of REST in small satellite cells abutting the neurons (Fig. 5 *A*1 and *A*2, red arrows) and also in dense intranuclear structures of most neurons (black arrows). Identical images were obtained with both Novus Biologicals antibodies and those kindly provided by G. Mandel.

In the second series of experiments, TG and brains from mice were harvested 7 d after infection or from untreated mice, solubilized, subjected to electrophoresis in a denaturing gel, and probed with antibody against REST. As shown in Fig. 5*B*, REST identified by its mass of ≈200 kDa was detected in TG of uninfected mice and in larger amounts in TG of mice infected with 10^5 pfu of wild-type HSV-1(F) virus administered by the corneal route. REST was barely detectable in brains of infected mice (Fig. 5*B*, lane 4, arrowhead). The 150-kDa band reactive with the anti-REST antibody in Fig. 5*B*, lane 4, was not reproducible, and could reflect a cross-reacting protein.

In the third series of experiments, the spleen, brains, and TG of uninfected mice and the TG of mice harvested 7 d after infection by the corneal route with 10^5 pfu of R111, R112, or wild-type parent virus were solubilized, subjected to electrophoresis in denaturing gels, and reacted with anti-REST antibody. The salient features of the results shown in Fig. 5*C* were as follows.

The 200-kDa REST was readily detected in all samples except the brain and ganglia of mice infected with the R112 recombinant virus.

Lysates of TG of mice infected with the R112 mutant contained a band reactive with anti-REST antibody that migrated with an electrophoretic mobility slightly faster than that of a protein with a mass of 150 kDa.

In these experiments, we consistently detected REST in TG by immunohistochemistry or by immunoblotting lysates. We did not detect REST in brains of uninfected mice. Trace amounts of REST were detected in brains of infected mice, consistent with the report that REST is detected following stress (11). Last, in TG of infected mice, REST was elevated in one experiment but not in another. We also note the absence of full-length REST in TG of infected mice. These differences may reflect effects of stress on the turnover of REST (12–14).

Relative Virulence of Wild-Type and Mutant Viruses. Titrations in mice by intracerebral route failed to yield significant differences between wild-type and mutant viruses with respect to the amount of virus required to cause lethal infection. Inoculation of groups of six mice per dilution by i.p. route indicated that R112 mutant virus was more virulent than its parent or the other recombinant viruses used in these studies. Thus, 100 pfu of R112 recombinant virus killed all six mice in this group. By contrast, the pfu/LD_{50} of wild-type or R111 or R113 mutant viruses were estimated to be significantly more than 1,000 pfu.

Discussion

Studies in cell culture predict that in nonneuronal cells at the portal of entry of virus into the body, HSV-1 overcomes the attempts to silence the genome by a repressor complex consisting of HDAC1 or 2, CoREST, REST, LSD1, and so forth. Current data support the model that ICP0, a viral α protein, binds to CoREST and displaces the HDACs from the repressor complex. Components of the complex are then transported to the cytoplasm (7, 8). From the portal of entry into the body, HSV-1 enters dorsal root or autonomic neurons in which it can establish a silent infection. The hypothesis we wished to test is that in neurons the silencing of the viral genome—a hallmark of latent HSV infection—is the result of repression by the same repressor complex

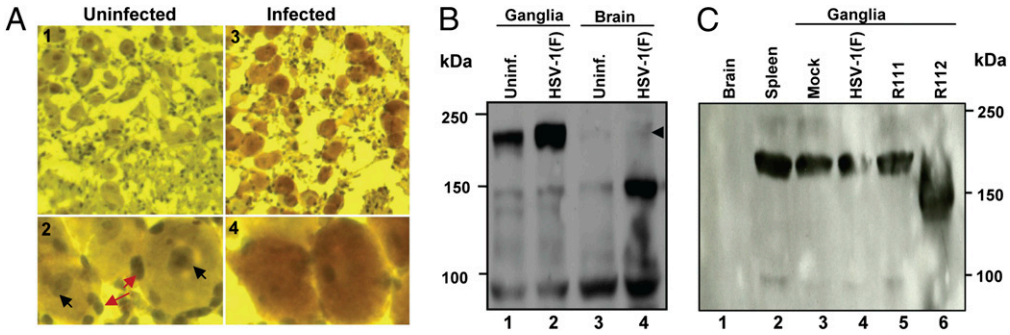

Fig. 5. Expression of REST in TG of mice inoculated with the R112 recombinant virus. (*A*) TG were removed from uninfected mice or from mice on day 7 after infection with 10^5 pfu of R112 virus, fixed, sectioned, and stained with anti-REST antibody (Novus Biologicals) as detailed in *Materials and Methods*. Virtually identical images were observed with antibody to REST kindly provided by G. Mandel. (*A*1 and *A*2) Low- (100× optics) and high- (400× optics) magnification photographs of TG from uninfected mice. (*A*3 and *A*4) Corresponding low- and high-magnification photographs of TG harvested from mice 7 d after corneal inoculation. Red and black arrow points to REST in satellite cells and in dense intranuclear structures in neuronal cells, respectively. (*B*) At 7 d postinfection, 10 ganglia from uninfected or HSV-1(F)-infected mice were pooled, washed, and lysed in RIPA buffer. One hundred micrograms of total protein lysates was loaded onto 8% SDS/PAGE, transferred to PVDF membrane, and Western-blotted with anti-REST antibody (Novus Biologicals). (*C*) At 7 d postinfection, brain and spleen from uninfected mice and 10 ganglia from uninfected or HSV-1(F)-, R111-, and R112-infected mice were harvested and processed as described in *B*. One hundred micrograms of total protein lysates was loaded onto 7.5% SDS/PAGE, transferred to PVDF membrane, and Western-blotted with anti-REST antibody (Novus Biologicals).

that fails to repress the genome in nonneuronal cells. Consistent with this hypothesis are reports that virus reactivation from latent state is enhanced by HDAC inhibitors (15–17). To test the hypothesis, we inserted a gene encoding REST devoid of both N- and C-terminal repressor domains into the wild-type HSV-1 genome. The expectation was that, if the silencing mechanism is the same as that encountered by the virus in nonneuronal cells, the dnREST expressed by the gene inserted into the wild-type genome would compete with resident REST protein and block silencing, as schematically depicted in Fig. 6*A*.

The results presented here show that the virus encoding the dnREST replicated to higher titers in the eye, TG, and brain than the wild-type parent or the virus expressing wild-type REST. As predicted, the DNA copy number of dnREST virus measured during the infectious phase of infected TG (days 1–14 after inoculation) was higher than that of other viruses. Finally, the virus carrying the dnREST gene was more virulent than the wild-type parent or the recombinant virus carrying wild-type REST. The increased virulence was reflected in higher mortality of virus delivered by the corneal or i.p. routes. None of the mice inoculated with the same dose of wild-type parent or other recombinants used in this study succumbed to infection. Wild-type REST at best could be expected to reinforce silencing and, indeed, the virus expressing wild-type REST could not be differentiated from the wild-type parent virus. To our knowledge, the functions conserved in the dnREST are nuclear localization and binding to DNA. The results reported here, a key test of the silencing hypothesis, do not reject it. There are four issues, however, that need to be brought forth.

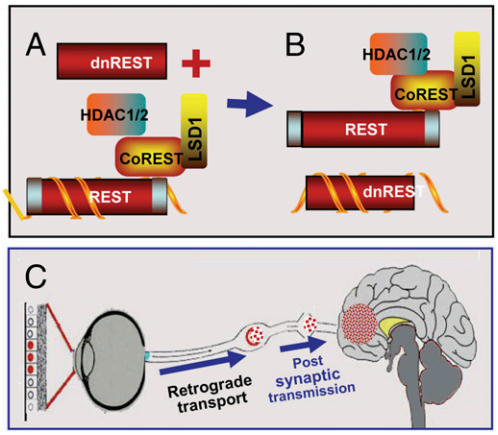

Fig. 6. Schematic representation of the suppression of silencing of HSV DNA by dnREST. (*A* and *B*) Components of the repressor complex are assembled on the DNA and silence the DNA. dnREST bound to DNA precludes the binding of corepressors from binding to dnREST. In *B*, dnREST binds to DNA and precludes the assembly of the repressor complex. (*C*) Schematic representation of translocation of virus from the cornea to the brain. The virus is transported retrograde to the neuronal ganglion. Normally, the virus would establish latency and on reactivation be transported anterograde to the portal of entry (cornea). In the studies performed with the R112 recombinant virus, extensive replication and destruction of the ganglia could lead to postsynaptic transmission of the virus to the brain. In light of detection of virus in the brain of asymptomatic mice, it is conceivable that small amounts of virus "leak" into the brain on reactivation but that these do not cause symptomatic disease.

(*i*) Increased virulence reflects a greater ability to replicate and spread to target organs before the mobilization of mouse adaptive immunity. This is particularly relevant in the case of virus replication in the eye that leads to seeding of TG with virus and in the case of virus inoculated by the i.p. route. The evidence that dnREST had such a profound effect on virulence suggests that (*a*) it interferes with the repression of viral DNA by cellular repressor complex containing wild-type REST and (*b*) cell cultures overstate the ability of wild-type virus to overcome the host silencing machinery in nonneuronal cells. Thus, the yields of R112 recombinant virus encoding dnREST in different cell lines were not significantly different from those of the wild-type virus or of other recombinants described in this report. Because the apparent function of dnREST is to thwart silencing, the evidence that the recombinant R112 is more virulent than the wild-type virus suggests that the latter is less efficient in blocking silencing in the cells it infects. This is not surprising: HSV is transmitted by physical contact of infected and uninfected tissues. Transmission of HSV causing excessive morbidity or mortality would be less frequent than that of virus causing mild symptoms of disease.

(*ii*) Although the results unambiguously demonstrate that dnREST enhanced viral replication in TG, the paramount question is how it acts. A compelling literature indicates that REST is a key component of a repressor complex that

MICROBIOLOGY

represses a large number of genes in nonneuronal cells (18, 19). In neuronal cells, active REST would be toxic. There is no universal agreement on the presence of REST in CNS neurons (20, 21). We failed to detect REST in brains of uninfected mice (Fig. 5*B*, lane 3 and Fig. 5*C*, lane 1). The failure to observe a greater virulence of R112 recombinant virus on intracerebral inoculation cited in *Results* is consistent with the absence of REST in uninfected brains. There was, however, an abundance of REST in TG of uninfected mice, chiefly in satellite cells and in dense structures in neuronal nuclei. Nevertheless, questions regarding REST remain. The results suggest that REST turns over (e.g., disappearance of wild-type REST in TG of mice infected with R112 or the failure of accumulation of large amounts of REST in TG of mice inoculated with R111 as apparent from the results shown in Fig. 5*C*, lanes 6 and 5, respectively), but the turnover rate and the activation of REST gene during infection remain to be elucidated.

(*iii*) Numerous reports attest to the ability of HSV to accumulate in detectable amounts in mouse brains without causing overt symptoms (e.g., 22). This phenomenon is illustrated with wild-type virus in Fig. 4. None of the mice inoculated by the eye route with wild-type virus succumbed to infection, and hence it is unlikely that the mice in which the virus was present in the brain would have succumbed to infection if they had been allowed to live. It is conceivable, although less likely, that the mice in which R112 recombinant virus was detected in the brain would also have survived. This conclusion is based on two observations. First, wild-type and R111 mutant viruses were detected in small amounts in brains at 5 and 7 d after corneal infection but not at later times. In contrast, the R112 mutant virus was detected in larger amounts as late as day 11 after infection. Second, the number of mice in which virus was detected exceeds the typical mortality rate observed in our studies with this virus. A central question is how the virus inoculated by the eye route reached the brain. One explanation is that the virus was transmitted from the eye to TG and from there to the brain. The eye infection smoldered for several days but was already in decline by day 7. The TG infection reached peak levels between days 7 and 14 and then declined. In the brain, the virus was detected on day 5 and reached the highest levels on day 9. Most mice succumbed to infection on days 11–14. The sequence of events favors the hypothesis that the rate of accretion of infectious virus along the way was triggered at least in part by the amount translocated at each step, from eye to TG and from TG by postsynaptic transmission to the brain. This route has been suggested in numerous publications (e.g., 23–25) and is illustrated in Fig. 6*B*. We cannot exclude the possibility that the virus was transmitted to the brain from lesions on the scalp that were readily apparent in several of the mice. However, the route from the skin to the brain is no less direct than that from TG.

(*iv*) It should be noted that murine ganglia containing latent virus also contain abundant viral microRNAs (26). It has been suggested that these microRNAs play a role in the establishment of latency by silencing viral DNA. Because many of the microRNAs are derived from the latency-associated transcripts, it is more likely that they may be involved in the maintenance rather than the establishment of the latent state.

Last, because the recombinant R112 has the potential of being more virulent to humans than wild-type strains, the properties of the virus were disclosed to the Institutional Biosafety Committee once the increased mortality of mice injected by the i.p. route became apparent. The studies of this virus were done under Biosafety Level 3 (BSL3) procedures in a restricted access BSL2 facility. R112 contains an intact thymidine kinase gene, and hence infections with this virus are amenable to antiviral treatment. Its potential as a bioweapon is limited by the requirement for physical contact between infected and uninfected tissues for successful transmission. The insertion of dnREST into the wild-type genome is not a universal path for increasing virus virulence because the mechanisms by which viruses block silencing by the host are likely to vary considerably. The R112 recombinant described in this report is likely to contribute significantly to our understanding of the mechanisms by which the host attempts to silence viruses—an important and not too well understood aspect of innate immunity—and the limitations that viruses have adopted to limit their virulence.

Materials and Methods

Viruses, Cells, and Antibodies. HSV-1(F), the BAC encoding the HSV-1(F) DNA, and Vero cells were reported elsewhere (8). Virus titrations were done on Vero cells. Antibodies against REST were from Novus Biologicals (NB100-910) and from G. Mandel.

Construction of Plasmids. Dominant-negative REST lacking residues 1–83 and 1008–1097 was obtained by linking two PCR fragments, n-REST and c-REST, through an SphI site. The n-REST fragment was PCR-amplified with primers 5′-CGGAATTCATGTTT T CAGATAGTGAAGAAGGAGAAGG-3′ and 5′-ACATGCATGCTCCATG GGAGGTGGCAGCTC CACC-3′. The c-REST fragment was PCR-amplified with primers 5′-ACATGCATGCTCAGATGGAGG GTGCCCAGATAC-3′ and 5′-CCCGACGTCTCATTATTCATCAATTTCCTGAGACTCATTTGC-3′. SV40 promoter and poly(A) signal were PCR-amplified and inserted into T-Easy vector to generate TV-40-poly(A). REST and dnREST were inserted, respectively, into TV-40-poly(A) in between SV40 promoter and poly(A) signal. The insert control was designed to replace REST by four stop codons (5′-TGATGATGATGA-3′). U_L3 gene was PCR-amplified with 5′-ACATGCATGCGC TAGCGGCGGCGTCCCACTC-TAGAATCGGTTGGA-3′ and 5′-CGGAATTCTCCCGG CCGGAT CGCGCTCGTCA-CCCGACA-3′ and ligated into T-Easy vector to generate TV-U_L3 plasmid. The U_L4 gene was PCR-amplified with 5′-ATAAGAATGCGGCCGCAGGCCTTCCTAGGAC-CCCA AAAGTTTGTCTGCGTAT-3′ and 5′-AACTGCAGGCTAGC ATGACCATCAC-GCGCTCCCAGG GCCTTAGC-3′ and ligated into T-U_L4 to generate TV-UL3-U_L4 plasmid. SV40-REST-poly(A), SV40-dnREST-poly(A), and SV40-4 STOP-poly(A) cassettes were inserted into TV-U_L3-U_L4 plasmid in between U_L3 and U_L4 to generate pY-REST, pY-dnREST, and pY-STOP plasmids, respectively. The fragments from PmeI digestion from pY-REST, pY-dnREST, and pY-STOP were cloned into pKO5 to generate pKO-111, pKO-112, and pKO-113.

Construction of Recombinant Viruses. Construction of BAC encoding REST, dnREST, and insertion control was done as reported elsewhere (8). Plasmid DNAs isolated from BAC-111, BAC-112, and BAC-113 were transfected into rabbit skin cells. Plaques obtained on rabbit skin cells were purified three times on Vero cells. Viral DNAs were isolated from individual plaques, and recombinant viruses R111, R112, and R113 were identified by PCR and sequenced to verify that no adventitious sequences were introduced during assembly of the recombinant viruses. The *tk* gene was rescued by cotransfection with a plasmid encoding the gene.

Inoculation of Mice. Five-week-old inbred female CBA/J mice (The Jackson Laboratory) received unrestricted access to food and water. The mice were inoculated with 5 μL of virus by the corneal route as described elsewhere (27). The studies were done in accordance with protocols approved by the Institutional Animal Use Committee.

DNA Isolation. Individual TG were digested with 100 μg of proteinase K in 500 μL of 50 mM Tris hydrochloride (pH 8.0), 100 mM EDTA, and 0.5% SDS overnight at 55 °C. The digested material was extracted with phenol/chloroform. The aqueous phases retained after centrifugation were pooled and extracted again with phenol/chloroform. The DNA was precipitated with ethanol overnight, collected by centrifugation, rinsed with 70% ethanol, dried, and suspended in 100 μL of distilled water. TG DNAs were standardized by optical density measurements.

Real-Time PCR Assays. Viral and cellular DNA copy numbers in TG were quantified by SYBR green real-time PCR technology (StepOnePlus System; Applied Biosystems) at an annealing temperature of 60 °C. The primers for viral thymidine kinase gene amplification were 5′-CTTAACAGCGTCAA-CAGCGTGCCG-3′ and 5′-CCAAAGAGGTGCGGGAG TTT-3′. The primers used for adipsin, the mouse single-copy gene, were 5′-AGTGTGCGGGGATGC AGT-3′ and 5′-ACGCGAGAGCCCCACGTA-3′.

Immunohistochemistry and Immunoblots. TG harvested at times indicated in the text were fixed in 4% paraformaldehyde for 12 h at 4 °C. Optimal cutting temperature (SKURA Inc.) was used for preparation of frozen TG at −80 °C for sectioning. Frozen TG were sliced 6 or 10 μm in thickness and stored at −80 °C. For staining, the sections were brought to room temperature, rinsed with PBS, reacted with antigen retrieval buffer (S1699; Dako), and heated in a steamer for 20 min over 97 °C. The slides were reacted with 3% H_2O_2 for 5 min, and then reacted with anti-REST antibody. Bound antibody was detected by Envision+ anti-rabbit system (K4002; Dako). The slides were briefly immersed in hematoxylin for counterstaining and evaluated under a light microscope. Immunoblots were done as described elsewhere (7, 8).

ACKNOWLEDGMENTS. We acknowledge with thanks the generous gift of reagents and numerous discussions with Gail Mandel (Oregon Health & Science University), the assistance of Lindsay Smith, and the work done by the DNA Sequencing and Immunohistochemistry facilities of the University of Chicago. These studies at the University of Chicago were aided by National Cancer Institute Grant 5R37CA078766-12 and a grant from the Cold Sore Foundation.

1. Roizman B, Knipe DM, Whitley RJ (2007) Herpes simplex viruses. *Fields Virology*, eds Knipe DM, et al. (Lippincott Williams & Wilkins, New York), 5th Ed, pp 2501–2601.
2. Liang Y, Vogel JL, Narayanan A, Peng H, Kristie TM (2009) Inhibition of the histone demethylase LSD1 blocks α-herpesvirus lytic replication and reactivation from latency. *Nat Med* 15:1312–1317.
3. Chen J, Panagiotidis C, Silverstein S (1992) Multimerization of ICP0, a herpes simplex virus immediate-early protein. *J Virol* 66:5598–5602.
4. Everett RD, Boutell C, Orr A (2004) Phenotype of a herpes simplex virus type 1 mutant that fails to express immediate-early regulatory protein ICP0. *J Virol* 78:1763–1774.
5. Ballas N, Mandel G (2005) The many faces of REST oversee epigenetic programming of neuronal genes. *Curr Opin Neurobiol* 15:500–506.
6. Gopalakrishnan V (2009) REST and the RESTless: In stem cells and beyond. *Future Neurol* 4:317–329.
7. Gu H, Liang Y, Mandel G, Roizman B (2005) Components of the REST/CoREST/histone deacetylase repressor complex are disrupted, modified, and translocated in HSV-1-infected cells. *Proc Natl Acad Sci USA* 102:7571–7576.
8. Gu H, Roizman B (2007) Herpes simplex virus-infected cell protein 0 blocks the silencing of viral DNA by dissociating histone deacetylases from the CoREST-REST complex. *Proc Natl Acad Sci USA* 104:17134–17139.
9. Poon AP, Gu H, Roizman B (2006) ICP0 and the US3 protein kinase of herpes simplex virus 1 independently block histone deacetylation to enable gene expression. *Proc Natl Acad Sci USA* 103:9993–9998.
10. Tapia-Ramírez J, Eggen BJ, Peral-Rubio MJ, Toledo-Aral JJ, Mandel G (1997) A single zinc finger motif in the silencing factor REST represses the neural-specific type II sodium channel promoter. *Proc Natl Acad Sci USA* 94:1177–1182.
11. Calderone A, et al. (2003) Ischemic insults derepress the gene silencer REST in neurons destined to die. *J Neurosci* 23:2112–2121.
12. Palm K, Belluardo N, Metsis M, Timmusk T (1998) Neuronal expression of zinc finger transcription factor REST/NRSF/XBR gene. *J Neurosci* 18:1280–1296.
13. Westbrook TF, et al. (2008) SCFβ-TRCP controls oncogenic transformation and neural differentiation through REST degradation. *Nature* 452:370–374.
14. Guardavaccaro D, et al. (2008) Control of chromosome stability by the β-TrCP-REST-Mad2 axis. *Nature* 452:365–369.
15. Danaher RJ, et al. (2005) Histone deacetylase inhibitors induce reactivation of herpes simplex virus type 1 in a latency-associated transcript-independent manner in neuronal cells. *J Neurovirol* 11:306–317.
16. Amelio AL, Giordani NV, Kubat NJ, O'Neil JE, Bloom DC (2006) Deacetylation of the herpes simplex virus type 1 latency-associated transcript (LAT) enhancer and a decrease in LAT abundance precede an increase in ICP0 transcriptional permissiveness at early times postexplant. *J Virol* 80:2063–2068.
17. Neumann DM, Bhattacharjee PS, Giordani NV, Bloom DC, Hill JM (2007) In vivo changes in the patterns of chromatin structure associated with the latent herpes simplex virus type 1 genome in mouse trigeminal ganglia can be detected at early times after butyrate treatment. *J Virol* 81:13248–13253.
18. Jothi R, Cuddapah S, Barski A, Cui K, Zhao K (2008) Genome-wide identification of in vivo protein-DNA binding sites from ChIP-Seq data. *Nucleic Acids Res* 36:5221–5231.
19. Johnson DS, Mortazavi A, Myers RM, Wold B (2007) Genome-wide mapping of in vivo protein-DNA interactions. *Science* 316:1497–1502.
20. Ballas N, Grunseich C, Lu DD, Speh JC, Mandel G (2005) REST and its corepressors mediate plasticity of neuronal gene chromatin throughout neurogenesis. *Cell* 121: 645–657.
21. Johnson R, Buckley NJ (2009) Gene dysregulation in Huntington's disease: REST, microRNAs and beyond. *Neuromolecular Med* 11:183–199.
22. Kümel G, et al. (1982) Experimental infection of inbred mice with herpes simplex virus. V. Investigations with a virus strain non-lethal after peripheral infection. *J Gen Virol* 63:315–323.
23. Davis LE, Johnson RT (1979) An explanation for the localization of herpes simplex encephalitis? *Ann Neurol* 5:2–5.
24. Esiri MM, Tomlinson AH (1984) Herpes simplex encephalitis. Immunohistological demonstration of spread of virus via olfactory and trigeminal pathways after infection of facial skin in mice. *J Neurol Sci* 64:213–217.
25. Margolis TP, LaVail JH, Setzer PY, Dawson CR (1989) Selective spread of herpes simplex virus in the central nervous system after ocular inoculation. *J Virol* 63: 4756–4761.
26. Umbach JL, et al. (2008) MicroRNAs expressed by herpes simplex virus 1 during latent infection regulate viral mRNAs. *Nature* 454:780–783.
27. Lagunoff M, Randall G, Roizman B (1996) Phenotypic properties of herpes simplex virus 1 containing a derepressed open reading frame P gene. *J Virol* 70:1810–1817.